J1.4 ANALYSIS OF THE N ALABAMA MCV ON THE MORNING OF 27 APRIL 2011

Stephanie Mullins* and Kevin Knupp
University of Alabama in Huntsville, Huntsville, AL

1. INTRODUCTION

On the morning of 27 April 2011, before the historic supercell outbreak of the afternoon, the first of two quasi-linear convective systems (QLCSs) progressed across N Alabama. As the line traversed Walker County, a prominent mesoscale convective vortex (MCV) became apparent from the NWS 88-D radars in Huntsville and Birmingham (KHTX and KBMX, respectively). The center of the MCV crossed Interstate 65 in Cullman County at about 11 UTC (6 am CDT). By 13 UTC, it had passed out of Alabama, crossed into extreme NW Georgia and into S Tennessee.

More than a dozen tornadoes occurred in association with the MCV, most notably impacting the Lake Guntersville State Park area and Marshall County (Fig. 1). For about an hour, dual-Doppler sampling was accomplished by KHTX and UAHuntsville's ARMOR (Advanced Radar for Meteorological and Operation Research). The geometry of the MCV in the ARMOR-KHTX dual-Doppler lobes (Fig. 2) allows for diagnosis of the 3-D wind field and associated circulations, and an assessment of the dual-polarimetric parameters observed by ARMOR.

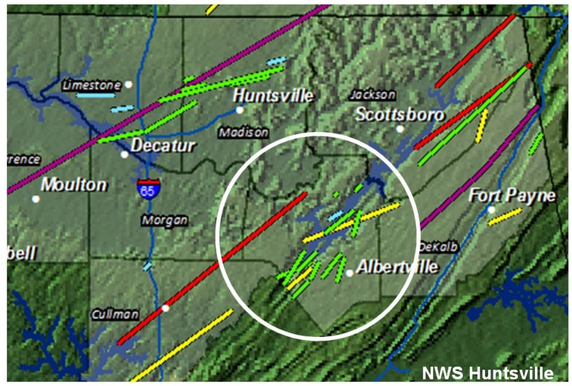

Fig. 1. Tracks of tornadoes on 27 April 2011 with Marshall County indicated by the white circle.

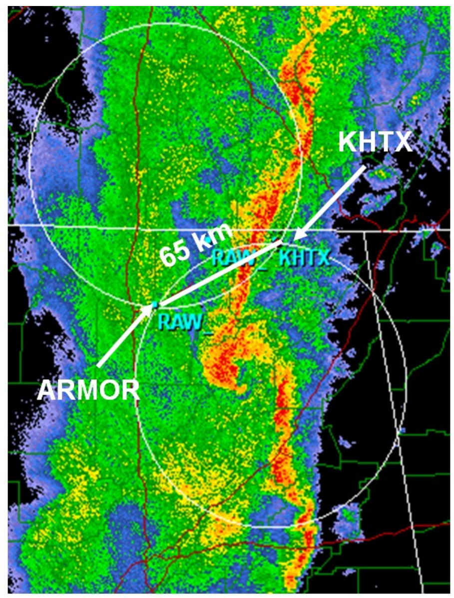

Fig. 2. 1145 UTC KHTX reflectivity. Radars and baseline are indicated. MCV is in the SE ARMOR-KHTX dual-Doppler lobe.

2. DATA & METHODOLOGY

For this study, super-resolution level II data from KHTX, which operated in VCP 212 collecting full volume scans, was used with data from ARMOR. ARMOR is a C-band, dual-polarization Doppler radar situated about 65 km to the WSW of KHTX; it is located at the Huntsville International Airport. During the MCV passage, ARMOR scanning alternated between a series of low-level 360° operational scans and sector volume scans of the MCV. The latter are used here, as the operational scans do not sample above 2.0° elevation.

The method employed is fairly straightforward and well used in the field for dual-Doppler radar analysis. Initial data from both radars was transferred to sweepfile format (Lee et al. 1994) and edited using NCAR's SoloII software, mainly to remove aliased velocities. Edited data were then gridded with REORDER (Oye et al. 1995) to a common Cartesian grid 100 x 100 x 15 km with horizontal and vertical spacing of 1.0 and 0.5 km, respectively.

Synthesis of radial wind components was completed in CEDRIC (Mohr et al. 1986). Vertical motion was found by integrating the continuity equation with a variational scheme with both upper and lower boundary conditions. Bulk estimates of hydrometeor fallspeed (v_t), derived from the maximum reflectivity (Z) value at each grid point, were then used to arrive at vertical air velocity, w

***Corresponding author address:** Stephanie Mullins, UAHuntsville ATS, NSSTC, 320 Sparkman Dr., Huntsville, AL, 35805; e-mail: mullins@nsstc.uah.edu

(i.e., w = W - v_t). The derived 3-D wind field was then used to compute the horizontal convergence, divergence, and vertical vorticity.

An initial evaluation of the dual-polarimetric parameters was done based on the differential reflectivity (Z_{dr}), specific differential phase (K_{dp}), and correlation coefficient (ρ_{hv}) data. Finally, tornado paths in N Alabama from the morning event, 1120-1218 UTC, were taken from NWS HUN's storm surveys and mapped in conjunction with the MCV's vorticity cores found from the analysis to look for correlations.

3. RESULTS

Results from specific, representative analysis times will be shown in detail. Based on the full hour of analysis, the following aspects of the MCV are clear: (1) it contained multiple vorticity centers at various times, (2) vorticity cores from the N most convective cells along the attendant QLCS to the S advanced to the MCV and often merged with its vorticity area, (3) vertical velocity magnitudes are relatively weak and peak at about 4 km height, (4) spatially, the storm relative horizontal wind maximum migrates counter-clockwise with time, and (5) hydrometeor characteristics inferred from the dual-polarimetric data suggest some sorting of larger vs. smaller water drops.

At 1139 UTC, the MCV contained two prominent vorticity peaks, as shown in Fig. 3. Also evident at this time is the vorticity core associated with the N most cell from the southern line. The strongest storm-relative horizontal winds peak (at 30.4 m s^{-1}) to the NW of the vorticity centers at 1 km. Vertical cross sections intersecting the 1 km vorticity maxima (Fig. 4) show largest vertical motion magnitudes all below 10 m s^{-1} and located below 6-8 km. Values of Z ≥ 30 dBZ are limited to below 6-8 km. Vorticity values are concentrated in the low levels, maximized at 9.7 x 10^{-3} s^{-1} at 1 km.

In the next analysis, 1145 UTC (Fig. 5), the MCV itself contains one distinct vorticity core, and the N most core of the trailing line has progressed to the MCV's periphery. The maximum horizontal storm relative winds at 1 km have progressed to the N side. Vertically, the results are similar to the previous time, with large vorticity concentrated in the lowest levels and relatively weak vertical motion (< 8 m s^{-1} at all heights).

Transitioning to 1149 UTC, the merger of the cell to the S with the MCV is clear in the vorticity field (Fig. 6), and the storm relative horizontal wind peak continues counter-clockwise,

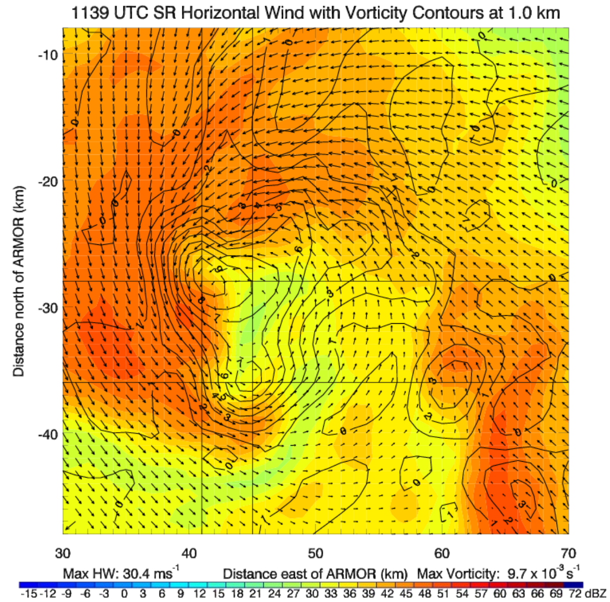

Fig. 3. 1139 UTC 1 km vertical vorticity (contoured, x 10^{-3} s^{-1}, largest value indicated at bottom right) and storm relative horizontal wind (vectors, "x" marker at highest value, magnitude indicated bottom left) over Z (shaded). Horizontal and vertical lines show locations of the vertical cross sections in Fig. 4.

now sitting to the NW. In the vertical planes passing through the 1 km vorticity maximum, upward motion is again confined below 8 km, but reaches a slightly higher magnitude than at previous analysis times (10.3 m s^{-1}). Low levels remain the richest in vorticity, with a peak value of 10.7 x 10^{-3} s^{-1}.

Davis and Trier (2007) investigated MCVs from the Bow Echo and Mesoscale Convective Vortex (BAMEX) field campaign. In each of their cases, the MCV developed from rotation embedded in the stratiform area of a mature MCS, in contrast to the MCV discussed here which formed from line end vortices along the QLCS. The horizontal scale of the BAMEX MCVs was also larger than that presented here. The 27 April MCV had a depth up to 8 km, similar to that found for BAMEX MCVs. In the latter cases, however, circulation was maximized aloft (550 - 600 hPa level), but here the largest vorticity was clearly concentrated at low levels.

As an example of the preliminary dual-polarimetric investigation, the ARMOR values for Z_{dr}, K_{dp}, and ρ_{hv} at 1145 UTC are provided in Fig. 7. First we will note that expected values of ρ_{hv} in rain are less at C-band than at S-band; thus the values from ARMOR correspond well to the presence of consistent targets. Negative values to

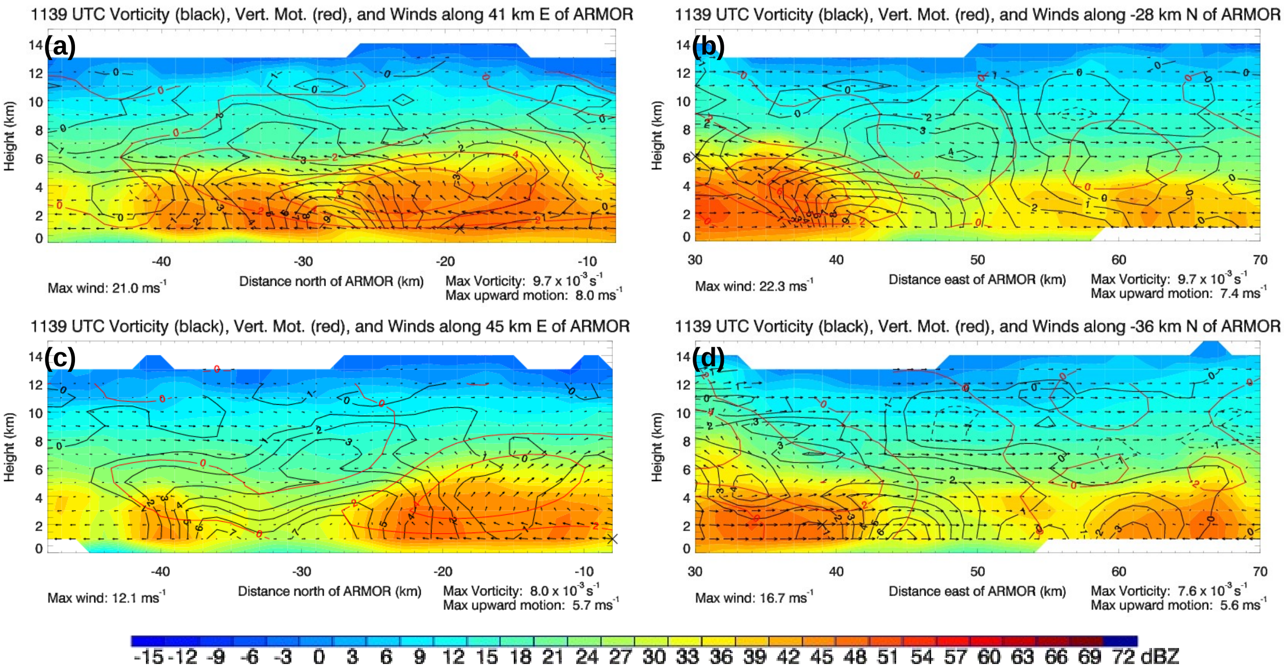

Fig. 4. Vertical cross sections along the lines indicated in Fig. 3. Vorticity (black contours, x 10^{-3} s^{-1}, largest value indicated at bottom right), vertical motion (red contours, m s^{-1}, largest value indicated at bottom right), and storm relative winds (vectors, "x" marker at highest value, magnitude indicated bottom left) over Z (shaded). (a) plane along 41 km E of ARMOR (E most line in Fig. 3), (b) plane along 28 km S of ARMOR (N most line in Fig. 3), (c) plane along 45 km E of ARMOR, (d) plane along 36 km S of ARMOR.

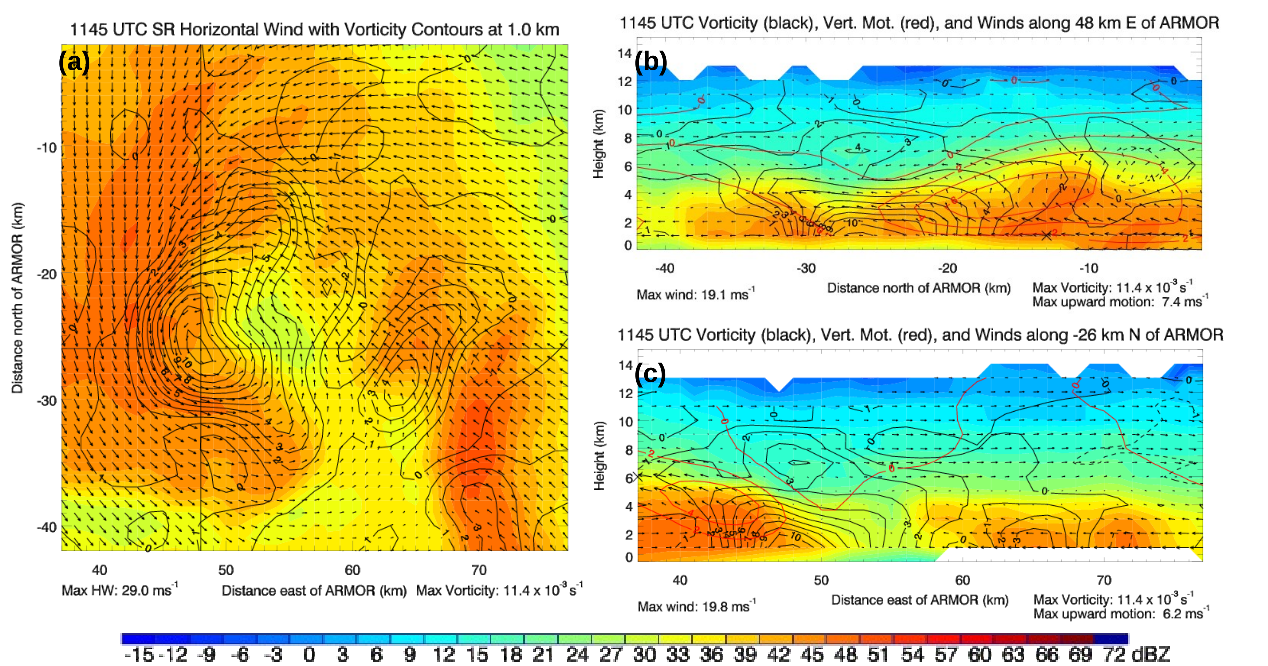

Fig. 5. As in Figs. 3 and 4. (a) 1145 UTC 1 km Z, vertical vorticity, and vertical motion, vertical sections through the (b) plane along 48 km E of ARMOR and (c) plane along 26 km S of ARMOR.

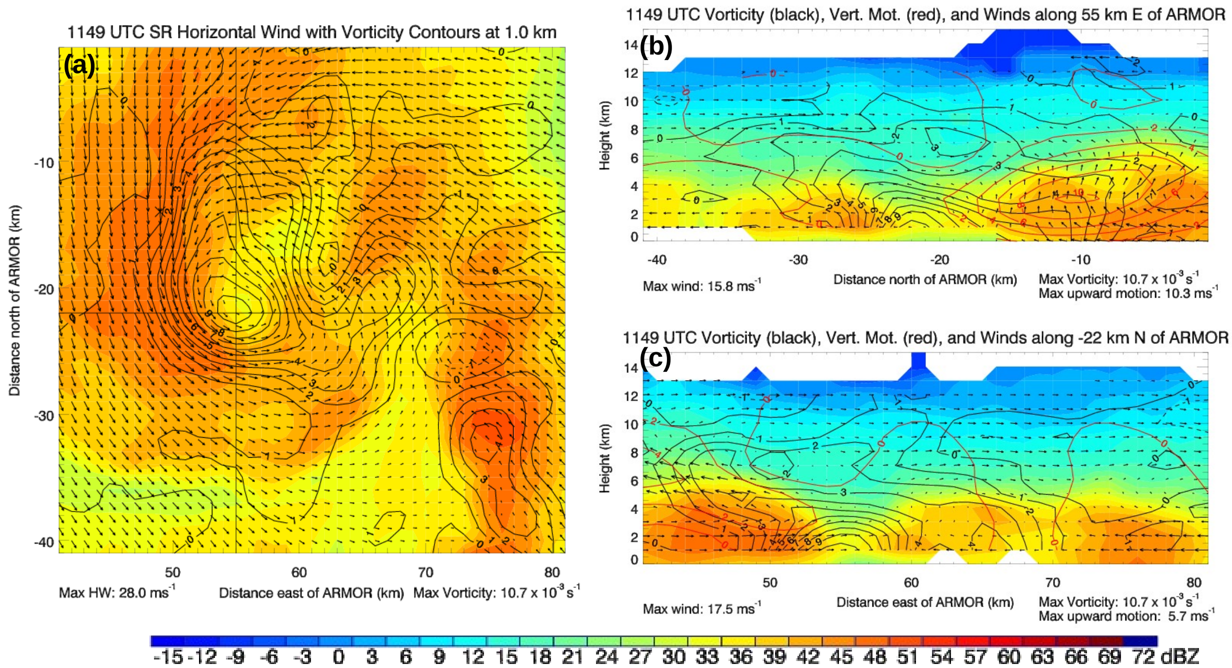

Fig. 6. As in Figs. 3 and 4. (a) 1149 UTC 1 km Z, vertical vorticity, and vertical motion, vertical sections through the (b) plane along 55 km E of ARMOR and (c) plane along 22 km S of ARMOR.

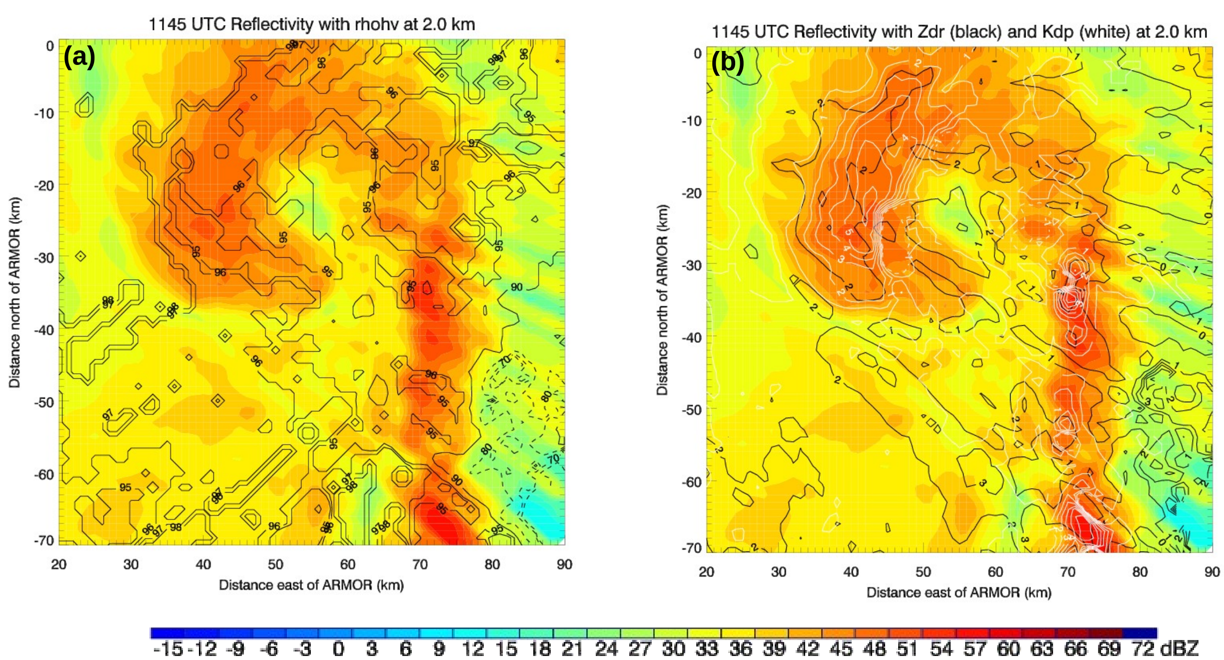

Fig. 7. 1145 UTC 2 km Z (shaded) with (a) correlation coefficient (black contours, as percent) and (b) differential reflectivity (black contours , dB), and specific differential phase (white contours, ° km^{-1}).

the E of the QLCS reflect attenuation on the far side of the echoes from the radar (ARMOR is located at 0,0 in the shown coordinate space). Z_{dr} values at the MCV center approach 0 dB as Z falls below 30 dBZ, indicating few, small raindrops. Along the W side of the MCV, bands of both Z_{dr} and K_{dp} are evident. Highest Z_{dr} values occur radially outward from the peak in K_{dp}. Larger, more oblate (higher valued Z_{dr}) raindrops are being sorted outward from the center of the MCV. Enhanced values of K_{dp} are related to increased liquid water content (Bringi and Chandrasekar 2001), so the maximum values ($\geq 6°$ km^{-1}) in the K_{dp} band (radially inward of the peak Z_{dr} values) point to a larger concentration of smaller drops, again indicating sorting of drops based on size.

4. COMPARISON TO TORNADO TRACKS

Tornado tracks were compiled by the NWS Huntsville staff's post-event storm surveys. Tracks for the morning tornadoes (start times 1120-1218 UTC) associated with the MCV, primarily in Marshall County, were mapped with vorticity contours for each analysis time. Results show very good visual correlation of vorticity cores to tornado track locations. Three examples are provided in Fig. 8. The MCV's main vorticity core remained throughout the analysis interval and also lines up well with the later, nearly 45 km long path, as indicated in the last panel.

5. SUMMARY

Dual-Doppler sampling of the MCV that traversed N Alabama on the morning of 27 April 2011 was achieved by the KHTX and ARMOR radars. As there were over a dozen tornadoes associated with it, detailed investigation of the MCV is instructive. Results from a full hour of dual-Doppler analysis and preliminary dual-polarimetric evaluation show that the MCV: (1) contained multiple strong ($> 9 \times 10^{-3}$ s^{-1}) vorticity centers confined to shallow layers generally under 3-4 km, (2) vorticity cores from the attendant QLCS to the S advanced to the MCV and often merged with its vorticity area, (3) vertical velocity magnitudes were relatively weak (< 10 m s^{-1}) and peaked at about 4 km height, (4) spatially, the storm relative horizontal wind maximum migrated counter-clockwise with time, (5) hydrometeor characteristics indicate sorting of larger vs. smaller water drops, and (6) vorticity centers were visually well aligned with several survey-determined EF-0 and EF-1 tornado tracks from the morning time frame.

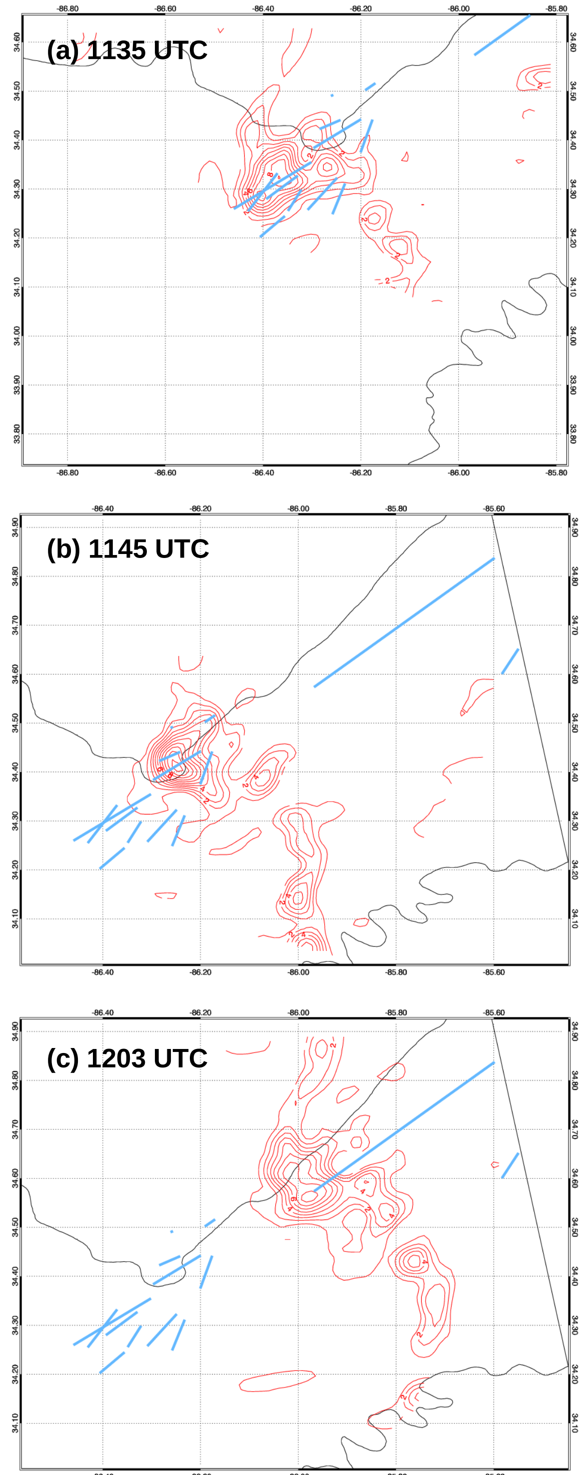

Fig. 8. Maps of EF-0 and EF-1 tornado tracks (blue) associated with the morning MCV passage with overlay of 1km positive vertical vorticity contours. (a) 1135, (b) 1145, and (c) 1203 UTC.

This initial study points to the need for continued work on this case. In addition to a more detailed look at the ARMOR dual-polarimetric data, single-Doppler radar analyses from KHTX as well as other NWS 88Ds will be useful to evaluate the development of the MCV with time and diagnose small scale circulations that are not resolvable with the dual-Doppler methodology. Results from such work can then be compared to those presented here, used for an evaluation of the MCV's dynamic balance, and perhaps to shed light on the origin of the robust low level vorticity shown over Marshall County.

6. ACKNOWLEDGMENTS

This study would not have been possible without Chris and Elise Schultz operating ARMOR in the morning on that fateful day. We would also like to thank the NWS WFO Huntsville staff, which did an excellent job completing the storm surveys, despite difficult circumstances, that identified the tornado paths. Funding for this project was provided by the NSF RAPID program under award AGS-1140387.

7. REFERENCES

Bringi, V.N., and V. Chandrasekar. 2001. *Polarimetric Doppler Weather Radar: Principles and Applications.* Cambridge University Press, 636 pp.

Davis, C.A., and S.B. Trier, 2007: Mesoscale Convective Vortices Observed during BAMEX. Part I: Kinematic and Thermodynamic Structure. *Mon. Wea. Rev.*, **135**, 2029–2049.

Lee, W., C. Walther, and R. Oye, 1994: Doppler Radar Data Exchange format DORADE. *NCAR Tech. Note, NCAR/TN-4031IA.*

Mohr, C.G., L.J. Miller, R.L. Vaughn, and H.W. Frank, 1986: The merger of mesoscale datasets into a common Cartesian format for efficient and systematic analyses. *J. Atmos. and Ocean. Tech.,* **3**, 143-161.

Oye, R., C. Mueller, and S. Smith, 1995: Software for radar translation, visualization, editing, and interpolation. *Preprints, 27th Conf. on Radar Meteorology*, Vail, CO, Amer. Meteor. Soc.